Anatomic–Functional Correlates in Lesions of Retinal Vein Occlusion

Meiaad Khayat,[1,2] Jennifer Perais,[1] David M. Wright,[3] Michael Williams,[4,5] and Noemi Lois[1,4]

[1]Wellcome-Wolfson Institute for Experimental Medicine, School of Medicine, Dentistry & Biomedical Sciences, Queen's University Belfast, United Kingdom
[2]The Department of Anatomy, Faculty of Medicine-Rabigh, King Abdulaziz University, Saudi Arabia
[3]The Centre for Public Health, School of Medicine, Dentistry & Biomedical Sciences, Queen's University Belfast, United Kingdom
[4]The Ophthalmology Department, The Belfast Health and Social Care Trust, Belfast, United Kingdom
[5]The Centre for Medical Education, School of Medicine, Dentistry & Biomedical Sciences, Queen's University Belfast, United Kingdom

Correspondence: Noemi Lois, Wellcome-Wolfson Center for Experimental Medicine, School of Medicine, Dentistry & Biomedical Sciences Queen's University Belfast, 97 Lisburn Road, BT9 5BW, Belfast, UK;
n.lois@qub.ac.uk.

Received: December 29, 2020
Accepted: May 12, 2021
Published: June 8, 2021

Citation: Khayat M, Perais J, Wright DM, Williams M, Lois N. Anatomic–functional correlates in lesions of retinal vein occlusion. *Invest Ophthalmol Vis Sci.* 2021;62(7):10. https://doi.org/10.1167/iovs.62.7.10

Purpose. To evaluate anatomic–functional associations at sites of retinal lesions in retinal vein occlusion (RVO).

Methods. This pilot, prospective, observational study was conducted at the Northern Ireland Clinical Research Facility (NICRF) of Queen's University and the Belfast Health and Social Care Trust, Northern Ireland, between August 1, 2018, and September 30, 2019. The study included 10 treatment-naïve patients with RVO (10 RVO eyes and 10 fellow eyes). There were 81 points/sites assessed for each eye at baseline; six patients were re-assessed 6 months after anti-vascular endothelial growth factor therapy at the same locations. We investigated associations between retinal sensitivity and presence of structural RVO lesions, including retinal ischemia, hemorrhages, intraretinal fluid (IRF) and subretinal fluid outside the foveal/parafoveal regions. Comparisons were made between RVO eyes and fellow eyes at baseline, and between RVO eyes at baseline and at 6 months after treatment. Regression models were used to investigate anatomic–functional associations.

Results. At baseline, strong associations were found between reduced retinal sensitivity and presence of ischemia (estimate = −2.08 dB; $P < 0.001$), intraretinal fluid (estimate = −7.82 dB; $P < 0.001$), and subretinal fluid (estimate = −8.66 dB; $P < 0.001$). Resolution of subretinal fluid but not intraretinal fluid was associated with improved function (estimate = 2.40 dB [$P = 0.022$]; estimate = 1.16 dB [$P = 0.228$], respectively). However, reperfusion of ischemic retina, observed in 31 of 486 points (6%) 6 months after anti-vascular endothelial growth factor therapy, was associated with a further decrease in retinal sensitivity (estimate = −2.34 dB; $P = 0.035$).

Conclusions. Retinal sensitivity was decreased at sites of RVO lesions. Decreased function at sites of retinal ischemia did not recover after treatment, even when reperfusion occurred.

Keywords: retina, retinal vein occlusion, RVO, anti-VEGF, vascular endothelial growth factor, macular edema, laser

Retinal vein occlusion (RVO) is phenotypically characterized by the presence of retinal hemorrhages, intraretinal and subretinal fluid (SRF) and a variable degree of retinal capillary nonperfusion (ischemia).[1,2] Distribution and extension of these RVO lesions varies depending on the type of RVO, whether central RVO (CRVO), branch RVO (BRVO), or hemispheric/hemicentral RVO. There is, to date, very scarce knowledge on the degree of functional loss that occurs as a result of these lesions and its potential reversibility after treatment.

Few studies have been conducted evaluating visual acuity and functional alterations, as determined by macular microperimetry, and their relationship with structural changes, as determined by spectral domain optical coherence tomography (SD-OCT) and fundus fluorescein angiography (FFA) or OCT angiography in eyes with RVO.[3–13] Studies undertaken have focused on the foveal and/or parafoveal regions[3–13]; some included only previously treated patients.[9–11] The different anatomy of the foveal/parafoveal region when compared with that outside it, the fact that this specialized retinal region is nourished by the choroid through the RPE besides through retinal blood vessels, and its high metabolic demand, makes it difficult to extrapolate findings to other areas of the retina. Most studies sought correlations between visual function (visual acuity and microperimetric parameters; e.g., fixation, mean

sensitivity values, scotoma size) and measures of retinal thickness on SD-OCT[3–6,8,12]; none evaluated the effect of anti-vascular endothelial growth factor (anti-VEGF) therapies on function/structure over specific retinal lesions of RVO. Very few studies pursued detailed point-to-point correlations in testing areas[7,9–11]; when done, these studies included previously treated patients, rather than those who were treatment naïve, who were tested once resolution of fluid had been achieved.[7,9–11] Most published studies were cross-sectional and, thus, unable to determine changes over time.[4–7,9-11,13]

Hence, the purpose of the current study was to meticulously evaluate point-to-point associations between retinal function and structural changes at the site of the various retinal lesions of RVO outside the fovea in treatment-naïve eyes, and to determine their reversibility 6 months after anti-VEGF therapy.

Methods

This pilot, prospective, observational study was undertaken at the Belfast Health and Social Care Trust (BHSCT), Belfast, Northern Ireland, between August 1, 2018, and September 30, 2019. Potential participants were identified through hospital referrals and/or while in clinic. Verbal and written information was provided and questions, if any, answered. Patients willing to take part provided informed consent before being recruited. Ethical and Trust approvals were in place (Reference No: 17159NL-AS/18/YH/0090). This study was conducted in accordance with the principles that have their origin in the Declaration of Helsinki.

Eligibility Criteria

Participants were considered eligible if they met the following inclusion criteria: adults (aged ≥18 years) with newly diagnosed, treatment-naïve, unilateral RVO (CRVO, BRVO, or hemispheric/hemicentral RVO), and who were able to understand and read English and provide informed consent. Patients who did not meet these inclusion criteria and those with other retinal diseases besides RVO or media opacities preventing adequate visualization of the retina were excluded.

Outcome Measures

Pointwise associations between retinal function (retinal sensitivity) and structural lesions of RVO, including retinal ischemia, hemorrhage, intraretinal fluid (IRF) and SRF at corresponding retinal locations at baseline were investigated. The influence of structural alterations, including presence/absence of the external limiting membrane (ELM) and inner segment/outer segment (IS/OS) layers, as well as total retinal thickness, and thickness of the Ganglion cell layer–inner plexiform layer (GCL-IPL), on retinal function was also evaluated. The relationship between resolution of RVO lesions and retinal function at 6 months after anti-VEGF therapy was sought. All patients had macular edema and were treated with either ranibizumab or aflibercept. The standard protocol for treatment includes an initial loading dose of three injections, each monthly, followed by a pro re nata regime until macular edema resolves.

Data Collection and Definitions Used

Demographics, medical and ophthalmic history, and medications used were recorded in purposely designed case report forms at baseline and updated, if required, at the 6-month follow-up assessment. All participants underwent a full clinical examination, undertaken by an optometrist and an ophthalmologist, at baseline and at the 6 ± 1-month follow-up visit. All tests were carried out at baseline and at follow-up in RVO affected eyes, but only once in fellow, contralateral eyes, which served as controls.

Best-corrected visual acuity, obtained after refraction, was measured using the Early Treatment Diabetic Retinopathy Study visual acuity charts at 4 m.

Slit-lamp biomicroscopy was undertaken. Then, ultra-wide field fundus imaging, including fundus and autofluorescence images and FFA were obtained in both, affected and unaffected fellow eyes, using the Optos California 200 Tx (Optos Dunfermline, Scotland, UK). For ultra-wide field FFA, an intravenous bolus of 1.5 mL of fluorescein (20%) dye was injected in a peripheral vein. Images were obtained in primary position (center field) in early, mid, and late phases of the angiogram in RVO eyes. The mid and late phases were obtained in fellow eyes as well. Once FFA was completed, patients were given a minimum rest of 30 minutes, to allow retinal recovery after photobleaching.

An area of retinal capillary nonperfusion (retinal ischemia) outside the fovea was identified and selected in the RVO eye. Then, the area to be tested for the purpose of the study was determined; this area contained part of the ischemic area, but also had to include an area of perfused retina. A testing area at the corresponding retinal location was also selected for the fellow eye. Then testing, as specified elsewhere in this article, continued.

Retinal sensitivity was measured in RVO and unaffected fellow eyes using macular microperimetry (MAIA macular integrity assessment, CenterVue, Padova, Italy). A custom-designed 8° × 8° square grid containing 81 stimuli (9 × 9 points), with a distance of 0.89° (approximately 270 µm) between points, was used. To ensure the study area selected based on FFA was fully tested with microperimetry, the FFA image was displayed on an Apple iPad 4.0 and visualized adjacent to the infrared image displayed by the MAIA. By comparing the images side by side, and using the optic disc and selected retinal vessels as landmarks, the MAIA 81-point grid was placed and testing started. Corresponding areas in fellow contralateral eyes were identified and selected as follows. A transparent sheet was used to trace/draw the selected location in the affected eye in relation to the optic disc, major retinal vessels and fovea, as displayed in the infrared retinal image of the affected eye on the MAIA screen. Then, the drawing was flipped to obtain what would correspond with the mirror image and location in the fellow eye. This image was then used to localize the area of testing in the displayed retinal image of the fellow eye shown by the MAIA. A training test was first performed to familiarize the participant with the microperimetry procedure. Then, after a rest, testing of study and fellow eyes was undertaken. For this purpose, a 4-2 threshold strategy and a standard Goldmann III stimulus size was used (duration of the stimulus: 200 ms; background luminance: 4 asb; maximum luminance: 1000 asb; stimulus dynamic range: 0–36 dB). Depending on the location of the area of interest, participants were asked to fixate either on a central target or at one of four targets on a ring around the center marked at the 2, 4, 8,

Investigative Ophthalmology & Visual Science

or 10 o'clock positions. The MAIA follow-up examination was used to ensure that repeated examinations in the same patient (i.e., baseline and 6-month follow-up) were undertaken at the exact same location. This function allows precise functional monitoring at different time points, even in cases where the retinal morphology has changed owing to pathology progression/regression.

SD-OCT and OCT-A images were obtained using a confocal scanning laser ophthalmoscope (Spectralis OCT, Heidelberg Engineering, Heidelberg, Germany). Positioning of the camera was adjusted to localize and cover the same area tested with microperimetry; optic disc and retinal vessels were used as landmarks to localize the area as accurately as possible. Depending on the location of the area of interest, participants were asked to fixate on either an internal or external target. A detailed high-resolution volume OCT test of 97 B-scans was obtained in an area of 10° × 15° (4.3 × 2.9 mm) of the retina with a distance of 30 µm between scans in SD-OCT. This customized densely packed OCT scan pattern was selected to ensure that structural data obtained could be mapped as best as possible to retinal sensitivity points. For OCT-A, a high-resolution volume test with 512 B-scans in an area of 10° × 10° (2.9 × 2.9 mm) of the retina with distance of 6 µm between B-scans was obtained at the area of interest. Automatic detection of the same area of testing was used to obtain SC-OCT and OCT-A images at the 6-month follow-up visit.

Data Processing and Alignment of Functional and Structural Data

Only patients who had areas of retinal ischemia that could be tested, owing to their location, with all other functional and imaging measurements, as detailed elsewhere in this article, were included in the analysis. Retinal sensitivity, an early arteriovenous phase FFA image (for the detection of retinal ischemia), SD-OCT scans (for detection of the IRF and SRF, integrity of the ELM and IS/OS layers, and total retinal thickness and thickness of the GCL-IPL), pseudocolor, and AF images (used to aid the interpretation of FFA and OCT features) were processed and superimposed, to make pointwise comparisons. OCT-A images of the superficial capillary plexus were used to assist in defining the area of retinal ischemia, as determined on FFA. Superimposing of all data was undertaking for three sets of measurements (RVO eyes at baseline and the 6-month follow-up, and fellow eyes).

Each of the retinal sensitivity points was given a unique label to help identify its location in the MAIA microperimetry grid. Each grid had nine rows and nine columns. For the RVO eye at baseline and 6 months follow-up, each row was assigned a letter from A to I and each column was assigned a number from 1 to 9 from left to right (e.g., point B3 is the point at the second row and third column from left to right). For the fellow eye, the numbering of the columns was reversed to be 9 to 1 from left to right (i.e., point B3 in the RVO affected eye will correspond with point B3 in the fellow control eye) (Fig. 1). Each of the 81 points (9 rows) from A1 to I9 in each tested eye was evaluated for the presence or absence of retinal ischemia, retinal hemorrhage, IRF, SRF, and intact, lost, or ungradable IS/OS and ELM layers. The IS/OS and ELM layers were graded as present/intact if they could be clearly seen and followed in SD-OCT scans; absent/lost if they could not be seen or followed in SD-OCT scans despite reasonable image quality; and ungradable when grading was not possible, owing to structural alterations present preventing their grading or owing to inadequate quality of the image. In addition, two rows from each grid in RVO eyes (18 points), one through the area of ischemia and one through perfused, nonischemic retina, were also assessed for total retinal thickness and thickness of GCL-IPL in micrometers on SD-OCT.

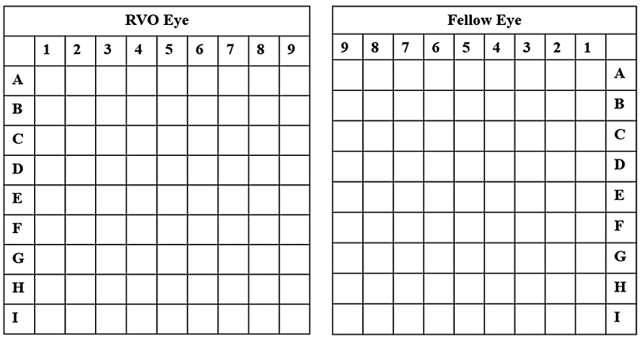

Figure 1. Labelling the locations of the retinal sensitivity points in the microperimetry grids for right and left eye.

Correlations at corresponding retinal locations between retinal sensitivity (dB) and lesions from RVO were then sought by superimposing retinal sensitivity values at the 81 different locations onto imaging data at the same locations. Manual processing and superimposition of the sensitivity maps and images from all technologies was executed using Microsoft Office 365 PowerPoint.

The superimposition of retinal images, including ultrawide field fundus and AF images and FFA, with the retinal sensitivity grid required several steps of preparation before analysis, including (1) enhancing images (contrast/brightness); (2) selection of the area corresponding with the retinal sensitivity grid (full 1024 × 1024 pixels infrared image); (3) cropping the selected area to be analyzed; (4) resizing of the image to match the retinal sensitivity grid; (5) identifying and positioning the retinal sensitivity grid over each of the three types of images (one at a time); and (6) a second cropping, required to ensure the area observed in the images was corresponding exactly to the retinal sensitivity grid (Figs. 2 and 3). The SD-OCT images required also similar preparation steps before they could be superimposed onto the retinal sensitivity grid (Fig. 4).

Statistical Analysis

The statistical analysis software IBM SPSS (Statistical Package for the Social Sciences), v24 was used to produce descriptive statistics. Associations between retinal sensitivity and lesions of RVO were investigated using the *R* software environment (The R Foundation for Statistical Computing, Vienna, Austria, version 3.4.3). Mixed-effects linear regression models were fitted to estimate associations between retinal sensitivity (function) and RVO lesions (structure), including the presence/absence of retinal ischemia, retinal hemorrhage, IRF, SRF, and the integrity of the ELM and IS/OS layer. All analyses were of complete cases (at the point level); points where imaging measurements were taken but ungradable points were included. A random effect term was used to represent the variation in retinal sensitivity among included patients and fixed effects were used for structural parameters. This model included all baseline measurements for

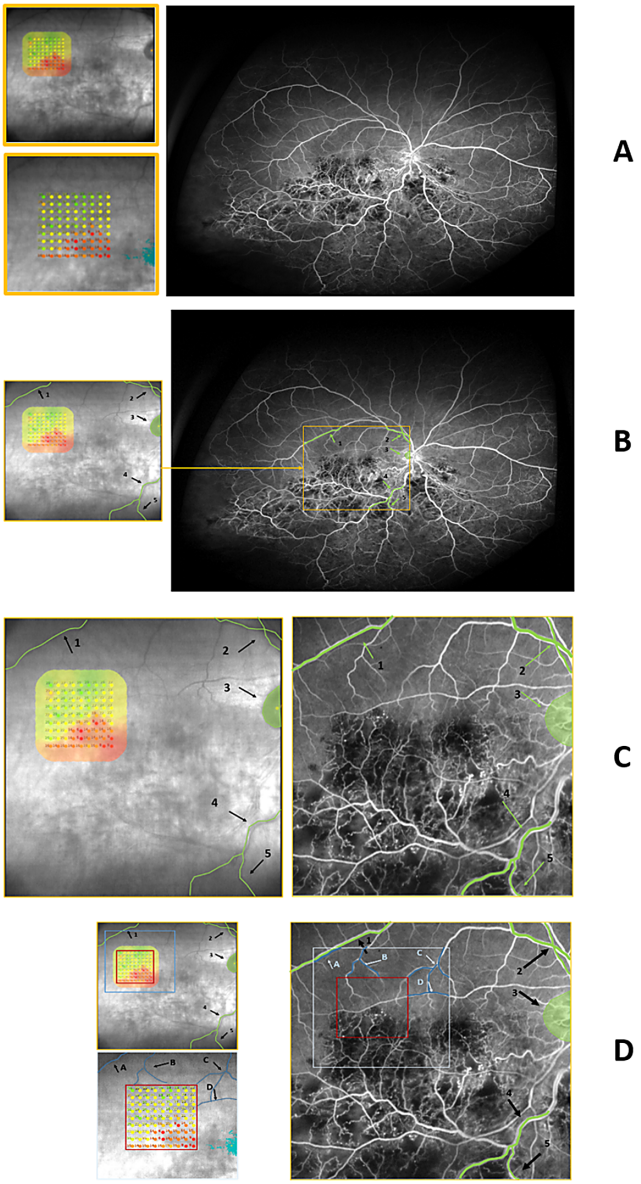

Figure 2. Processing of the retinal sensitivity map and wide-angle FFA (WA-FFA). Reference retinal sensitivity map (*top left*), sensitivity map (*bottom left*) and WA-FFA of the corresponding RVO eye (*right*) (**A**). Localization of the reference sensitivity map on WA-FFA (*yellow square*) using five landmarks (*highlighted in green*). Reference sensitivity map (*left*); WA-FFA (*right*) (**B**). Cropping the area of WA-FFA (*right*) corresponding to the reference retinal sensitivity map (*left*) (**C**). Localization of the retinal sensitivity points from the reference retinal sensitivity map (*top left*) and sensitivity map (*bottom left*) on cropped WA-FFA using landmarks (*highlighted in blue*) (**A**, **B**, **C** and **D**) close to the sensitivity grid (*red square*) (**D**). The white square represents the location of the sensitivity map image.

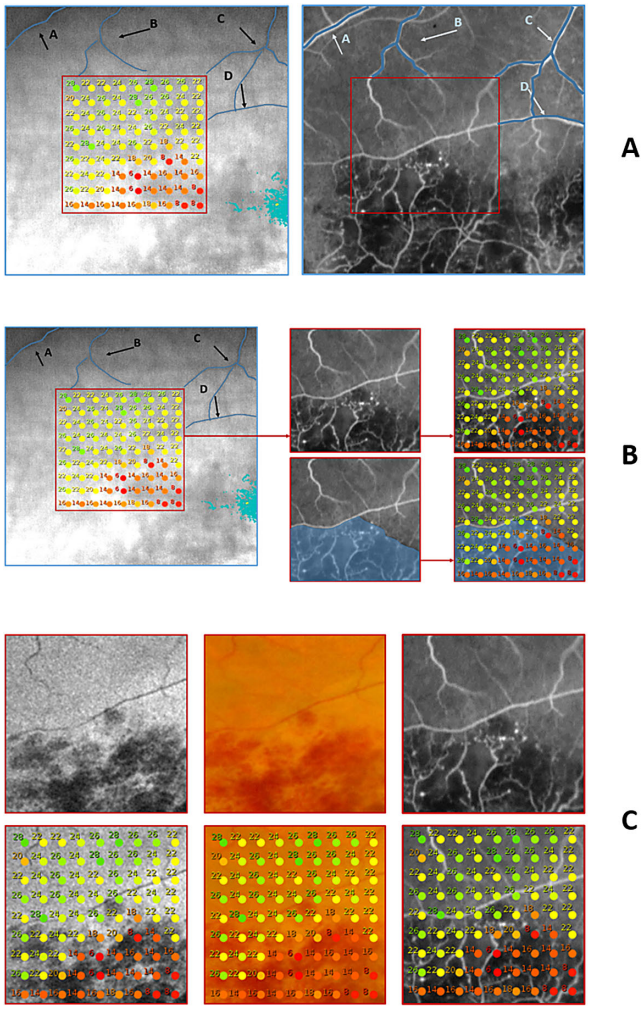

Figure 3. Superimposition of retinal sensitivity map and wide-angle FFA (WA-FFA). Cropped WA-FFA (*right*) corresponding with the retinal sensitivity map image (*left*). Landmarks are highlighted in blue in both images (**A**, **B**, **C**, and **D**) (**A**). Highlighting areas with retina ischemia (*blue*) on processed WA-FFA images and superimposing retinal sensitivity points on processed WA-FFA (*right*) images corresponding to retinal sensitivity map (*left*) (**B**). Superimposing the retinal sensitivity points on processed wide angle autofluorescence (AF) (*left*), fundus photography (*middle*), and WA-FFA (*right*) (**C**).

both affected and fellow eyes (a maximum of 162 points for each patient, 81 points from each eye). Lesion status was determined at the point level (rather than at the eye level). Fellow eyes contributed points with no lesions; affected eyes contributed with a mixture of points, some with lesions, some without them, with the proportion of points affected varying among lesion types (i.e., each point in an RVO eye would be classified as affected or unaffected and, if affected, whether there was hemorrhage, ischemia, SRF, IRF, etc., on it). Points within the same patient were not treated as independent observations; correlations within eyes were expected because points were close together; correlations between eyes were also expected because each patient was likely to have a given aptitude for the microperimetry testing. These dependencies were modelled using a single patient-level random effect that allowed patients to differ in their retinal sensitivity. Simultaneously, the effect of interest—the average difference in sensitivity across all eyes between points with lesions and those without lesions—was estimated in the fixed effects part of the model. Therefore, the reported coefficients denote the difference in sensitivity between points with lesions and those without lesions, accounting for differences among patients in test aptitude and for the different retinal regions sampled, with a large number of normal points provided by fellow eyes.

To quantify the relationship between retinal sensitivity and total retinal thickness as well as the thickness of the

Investigative Ophthalmology & Visual Science

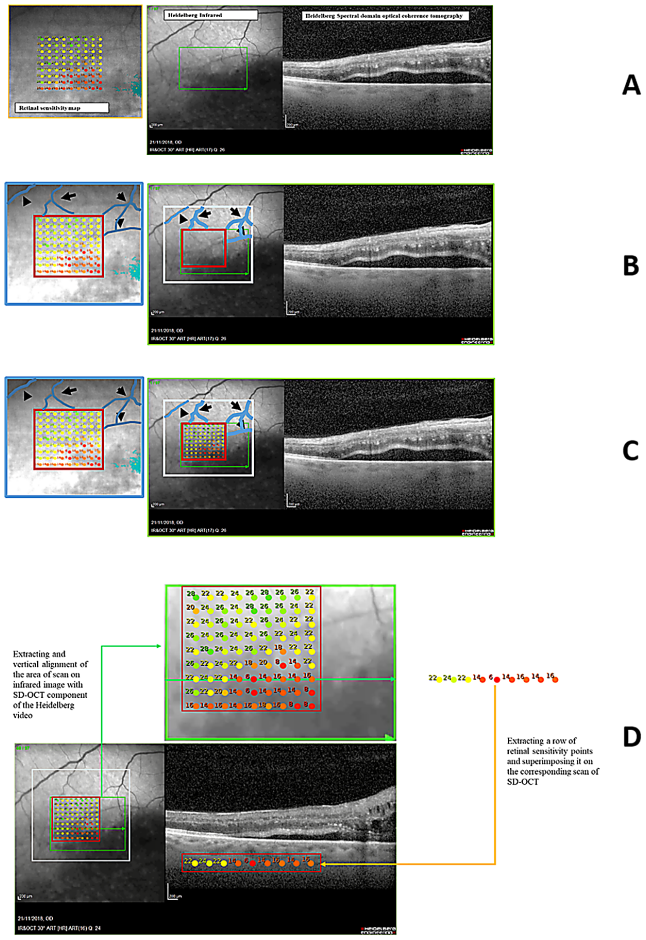

Figure 4. Processing and superimposition retinal sensitivity map and spectral domain FFA (SD-OCT). Retinal sensitivity map (*left*) and corresponding Heidelberg OCT video shot (*right*) showing infrared and SD-OCT components (**A**). Identifying landmarks (*highlighted in blue*) on retinal sensitivity map (*left*) and on corresponding Heidelberg infrared image of OCT (*right*) and localization of the grid of retinal sensitivity points on it (*red square*) (**B**). The white square represents the location of the retinal sensitivity map. Superimposing retinal sensitivity points on Heidelberg infrared component of OCT after identifying the location of the grid of the sensitivity points on infrared image (**C**). Superimposing retinal sensitivity points on the corresponding SD-OCT scan (**D**). The area of scan on Heidelberg infrared component of the OCT video (*green rectangle*) is extracted and aligned vertically with the SD-OCT component to identify the location of the sensitivity points. Each row of the retinal sensitivity points was matched with its corresponding SD-OCT scan. An example of the third row from the bottom (*row G*) is shown.

GCL-IPL, separate regressions were fitted for the subset of points in which these measurements were taken. A regression was fitted for each variable, added as a fixed effect to the previous model of retinal sensitivity at baseline. Before undertaking model fitting, thickness measures were standardized by subtracting the mean and dividing by the standard deviation (μm). Statistical significance was considered when the P was less than 0.05.

A separate analysis was conducted to evaluate the relationships between the change in retinal sensitivity from baseline to 6 months and the various RVO lesions. Only affected eyes were included. Comparisons were made at the pointwise level explicitly comparing sensitivity at the exact same location in the affected eye at baseline and the 6-month follow-up. The outcome variable (sensitivity difference) was calculated as: Affected eye at point x at baseline – affected eye at point x at the 6-month follow-up. A positive value would indicate improved sensitivity, whereas a negative value would indicate a deterioration. Statistical significance was considered when the P value was less than 0.05.

Results

Twelve patients were found to be eligible and recruited into the study; all underwent a baseline examination. Of these patients, 10 were found to have areas of retinal ischemia outside the fovea that could be reached and tested with all functional and imaging technologies and so were included in the analysis. The two patients excluded did not have areas of capillary nonperfusion accessible for testing (i.e., within 30° from the foveal center). Areas tested were located in the superotemporal aspect of the posterior pole ($n = 4$ [40%]), in the temporal aspect of the posterior pole ($n = 4$ [40%]), or in the inferotemporal aspect of the posterior pole ($n = 2$ [20%]), and in all cases outside the foveal area. A summary of demographics and characteristics of the 10 patients included in the analysis is shown in Table 1. The mean ± standard deviation number of anti-VEGF injections received was 3 ± 1.

Functional–Structural Associations at Baseline

The mean retinal sensitivity values at sites of retinal ischemia, hemorrhage, IRF, SRF, and loss of IS/OS and ELM layers when compared with sites without them in RVO eyes and fellow eyes at baseline (10 patients, 810 locations studied) are shown in Table 2. There was strong evidence that retinal sensitivity was lower in the presence of ischemia, hemorrhage, IRF, or SRF in affected eyes, when compared with points where these lesions were not present, and when compared with corresponding locations in fellow eyes. A mixed-effects linear regression analysis demonstrated the lowest retinal sensitivity occurred at points with IRF and SRF (−7.82 dB and −8.66 dB, respectively; $P < 0.001$ for each), and the sensitivity was −2.08 dB at points with ischemia ($P < 0.001$) and −1.23 dB at points with hemorrhage ($P = 0.020$) (Table 3). There was no association between integrity of the ELM and retinal sensitivity ($P = 0.644$), but there was evidence that the sensitivity was lower at locations where the ELM was labelled as ungradable ($P = 0.002$). It should be noted, however, that the number of points with absent ELM was small ($n = 22$). There was no association between the absence of the IS/OS and retinal sensitivity ($P = 0.468$), but there were only three points in this category.

The total retinal thickness and the thickness of the GCL-IPL, as recorded in 180 locations in 10 RVO eyes at sites with and without retinal ischemia, hemorrhage, IRF, SRF, IS/OS, and ELM layer and at corresponding sites in 10 fellow eyes, as well as corresponding values of retinal sensitivity, are shown in Table 4. A mixed-effects linear regression analysis demonstrated evidence of a negative association between total retinal thickness and retinal sensitivity ($P = 0.021$) (Table 5). The magnitude of the estimated association was found to be moderate, with a one standard deviation increase in thickness of total retina associated with a reduction in retinal sensitivity of −1.44 dB. Associations between retinal sensitivity and each of the different structural lesions of RVO remained when correcting for total

Investigative Ophthalmology & Visual Science

Table 1. Demographics and Patient Characteristics in Eyes With RVO ($n = 10$) and Fellow Eyes ($n = 10$) At Baseline

Characteristic/Measure		
Age (mean ± SD) years [range]	78 ± 6 [66–88]	
Gender (n) male: female	5: 5	
Type of RVO (n)		
CRVO	5/10	
HRVO	3/10	
BRVO	2/10	
Affected eye (n) left: right	7: 3	
Duration of symptoms (mea n ± SD), months [range]	4 ± 4 [1–9]	
Diabetes mellitus (n)	1/10	
Hypertension (n)	6/10	
Dyslipidemia (n)	9/10	
	RVO Eye at Baseline ($n = 10$)	Control Fellow Eye ($n = 10$)
Best corrected visual acuity (mean ± SD) ETDRS letters [range]	39 ± 17 [0–67]	76 ± 16 [38–89]
IOP (mean ± SD) mm Hg [range]	17 ± 5 [13–29]	17 ± 3 [12–21]
Macular edema (n)	10/10	0/10
Neovascularization (n)	0/10	0/10

ETDRS, Early Treatment Diabetic Retinopathy Study; HRVO, hemispheric/hemicentral RVO; SD, standard deviation.

Table 2. Retinal Sensitivity (Mean ± Standard Deviation) at Sites of Structural Lesions of RVO at Baseline (810 Total Pointed Studied) in Affected Eyes and Corresponding Values in Controls Eyes in 10 Patients with RVO

Anatomic Parameter	Retinal Sensitivity (dB) in RVO Eye (10 Eyes) ($n = 810$)				Retinal Sensitivity (dB) in Fellow Eye (10 Eyes) ($n = 810$)
Ischemia	Nonperfused (Ischemic) ($n = 313$) 13 ± 9	Perfused (nonischemic) ($n = 490$) 19 ± 8	Not available ($n = 7$)		24 ± 6
Hemorrhage	Present ($n = 145$) 14 ± 8	Absent ($n = 659$) 17 ± 9	Not available ($n = 6$)		24 ± 6
IRF	Present IRF ($n = 296$) 11 ± 8	Absent IRF ($n = 464$) 20 ± 7	Not available ($n = 50$)		24 ± 6
SRF	Present SRF ($n = 181$) 10 ± 6	Absent SRF ($n = 585$) 18 ± 8	Not available ($n = 44$)		24 ± 6
IS/OS	IS/OS - present ($n = 748$) 17 ± 8	IS/OS - absent ($n = 3$) 3 ± 5	IS/OS ungradable ($n = 24$) 3 ± 5	Not available ($n = 35$)	24 ± 6
ELM	ELM-present ($n = 636$) 18 ± 8	ELM - absent ($n = 22$) 7 ± 6	ELM - ungradable ($n = 117$) 7 ± 6	Not available ($n = 35$)	24 ± 6

retinal thickness, with the exception of hemorrhage, which no longer showed a statistically significant association with retinal sensitivity (Table 5). The relationship between retinal sensitivity and thickness of GCL-IPL was found to be similar and in the same direction as that observed for total retinal thickness ($P = 0.022$), with a 1-standard deviation increase

Table 3. Associations Between Retinal Sensitivity and Structural Lesions of RVO at Baseline in 10 RVO Eyes and 10 Fellow Eyes (1514 Points) (Mixed-Effects Linear Regression Model)

Term	Estimated Coefficient	Standard Error	t-Statistic	P Value
Overall mean (intercept)	23.22	1.21	19.18	<0.001
Ischemia - present	−2.08	0.41	−5.09	<0.001
Hemorrhage - present	−1.23	0.53	−2.33	0.020
IRF - present	−7.82	0.49	−15.98	<0.001
SRF - present	−8.66	0.56	−15.39	<0.001
IS/OS - ungradable	−0.82	1.31	−0.62	0.533
IS/OS - absent	−2.37	3.26	−0.73	0.468
ELM - ungradable	−2.68	0.86	−3.10	0.002
ELM - absent	0.62	1.33	0.46	0.644

Investigative Ophthalmology & Visual Science

Table 4. Retinal Sensitivity and Retinal Thicknesses (Mean ± Standard Deviation) Values at Sites of Structural Lesions of RVO in Affected (10 Eyes) and Fellow Eyes (10 Eyes) at Baseline

Parameter	**RVO Eye (10 Eyes) (n = 178)***			**Fellow Eye (10 Eyes) (n = 178)***
Ischemia	Nonperfused (Ischemic) (n = 59)	Perfused (nonischemic) (n = 116)	Not available (n = 3)	Control (n = 178)
Sensitivity (dB)	13 ± 9	18 ± 8	–	24 ± 6
Total thickness (µm)	421 ± 134	406 ± 159	562 ± 33	282 ± 60
GCL-IPL thickness (µm)	126 ± 95	124 ± 66	52 ± 3	86 ± 34
Hemorrhage	Present (n = 28)	Absent (n = 147)	Not available (n = 3)	Control (n = 178)
Sensitivity (dB)	16 ± 8	17 ± 9	–	24 ± 6
Total thickness (µm)	424 ± 123	408 ± 155	562 ± 33	282 ± 60
GCL-IPL thickness (µm)	126 ± 44	125 ± 82	52 ± 3	86 ± 34
IRF	Present IRF (n = 54)	Absent IRF (n = 121)	Not available (n = 3)	Control (n = 178)
Sensitivity (dB)	10 ± 7	20 ± 7	–	24 ± 6
Total thickness (µm)	576 ± 129	337 ± 87	562 ± 33	282 ± 60
GCL-IPL thickness (µm)	182 ± 1110	99 ± 32	52 ± 3	86 ± 34
SRF	Present SRF (n = 41)	Absent SRF (n = 137)	Not available (n = 0)	Control (n = 178)
Sensitivity (dB)	10 ± 7	19 ± 8	–	24 ± 6
Total thickness (µm)	545 ± 146	374 ± 128	–	282 ± 60
GCL-IPL thickness (µm)	166 ± 73	111 ± 74	–	86 ± 34
IS/OS	IS/OS - present (n = 174)	IS/OS - absent (n = 0)	IS/OS ungradable (n = 4)	Not available (n = 0)	Control (n = 178)
Sensitivity (dB)	17 ± 9	–	4 ± 3	–	24 ± 6
Total thickness (µm)	405 ± 1141	–	775 ± 89	–	282 ± 60
GCL-IPL thickness (µm)	118 ± 65	–	380 ± 127	–	86 ± 34
ELM	ELM - present (n = 152)	ELM - absent (n = 0)	ELM ungradable (n = 26)	Not available (n = 0)	Control (n = 178)
Sensitivity (dB)	18 ± 8	–	5 ± 4	–	24 ± 6
Total thickness (µm)	376 ± 120	–	631 ± 126	–	282 ± 60
GCL-IPL thickness (µm)	122 ± 66	–	133 ± 124	–	86 ± 34

*The 178 points rather than 180 points are presented as the two points at which sensitivity was tested dropped outside the scanned area.

Table 5. Associations Between Retinal Sensitivity and Structural Lesions of RVO at Baseline in 10 RVO Eyes and at Corresponding Locations in 10 Fellow Eyes (347 Points) Corrected for Total Retinal Thickness (Mixed-Effect Linear Regression Model)

Term	Estimated Coefficient	Standard Error	*t*-Statistic	*P* Value
Overall mean (intercept)	22.70	1.24	18.32	<0.001
Ischemia - present	−3.35	0.38	−4.04	<0.001
Hemorrhage - present	−0.09	1.15	−0.08	0.935
IRF - present	−6.14	1.29	−4.76	<0.001
SRF - present	−7.19	1.30	−5.52	<0.001
IS/OS - ungradable	1.90	3.05	−0.62	0.533
ELM - ungradable	−2.52	1.97	−1.28	0.201
Total retinal thickness (µm)	−1.44	0.62	−2.33	0.021

Table 6. Associations Between Retinal Sensitivity and Structural Parameters at Baseline (10 RVO Eyes and 10 Fellow Eyes, 347 Points) Corrected for GCL-IPL Thickness (Mixed-Effect Linear Regression Model)

Term	Estimated Coefficient	Standard Error	*t*-Statistic	*P* Value
Overall mean (intercept)	23.4	1.24	18.59	<0.001
Ischemia - present	−3.18	0.83	−3.82	<0.001
Hemorrhage - present	0.00	1.15	0.00	0.999
IRF - present	−6.39	1.24	−5.16	<0.001
SRF - present	−8.38	1.12	−7.48	<0.001
IS/OS - ungradable	5.71	3.43	1.66	0.097
ELM - ungradable	−5.52	1.86	−2.97	0.003
GCL-IPL thickness (µm)	−1.17	0.51	−2.30	0.022

in thickness of the GCL-IPL associated with a reduction in retinal sensitivity of −1.17 dB (Table 6).

Functional–Structural Correlations at 6 Months After Treatment

Retinal sensitivity values in eyes with RVO at sites where lesions persisted, resolved, or developed during the follow-up and at sites where they were absent at baseline and at 6 months (486 points studied) are shown in Table 7.

There was strong evidence that the development or persistence of retinal ischemia was associated with a more severe deterioration in retinal sensitivity when compared with the effect of other RVO lesions (Table 8). Locations in which retinal ischemia developed from baseline to the 6-month follow-up visit underwent more marked deterioration in sensitivity ($n = 44$) (−3.65 dB; $P < 0.001$), followed by those where ischemia persisted ($n = 158$) (−2.98 dB; $P < 0.001$). Even after resolution (i.e., retinal reperfusion in points with preexisting retinal ischemia at baseline), which occurred rarely ($n = 31$), retinal sensitivity remained below

Table 7. Changes in Retinal Sensitivity (Mean ± Standard Deviation) From Baseline to 6 Months at Sites of Structural Retinal Lesions of RVO in Six Patients (6 Eyes) at 486 Locations

Anatomic Parameter	Retinal Sensitivity (dB)				
	RVO eye ($n = 6$ patients, 6 eyes) ($n = 486$)				
Ischemia	Absent ($n = 237$)	Developed ($n = 44$)	Persisted ($n = 158$)	Resolved ($n = 31$)	Not available ($n = 16$)
Baseline sensitivity (dB)	17 ± 8	11 ± 9	11 ± 8	13 ± 8	–
Sensitivity change (dB)	5 ± 7	1 ± 11	−1 ± 8	−5 ± 8	–
Hemorrhage	($n = 363$)	($n = 1$)	($n = 2$)	($n = 114$)	($n = 6$)
Baseline sensitivity (dB)	15 ± 8	2	15 ± 1	12 ± 8	–
Sensitivity change (dB)	1 ± 8	20	4 ± 0	5 ± 8	–
IRF	($n = 214$)	($n = 0$)	($n = 0$)	($n = 240$)	($n = 32$)
Baseline sensitivity (dB)	21 ± 6	–	–	9 ± 6	–
Sensitivity change (dB)	1 ± 7	–	–	3 ± 10	–
SRF	($n = 346$)	($n = 0$)	($n = 0$)	($n = 114$)	($n = 26$)
Baseline sensitivity (dB)	16 ± 9	–	–	9 ± 6	–
Sensitivity change (dB)	0 ± 7	–	–	10 ± 6	–
IS/OS	Loss persisted ($n = 0$)	Loss resolved ($n = 3$)	Remained intact ($n = 433$)	Loss developed ($n = 0$)	Not available ($n = 50$)
Baseline sensitivity (dB)	–	5 ± 5	15 ± 8	–	–
Sensitivity change (dB)	–	13 ± 8	2 ± 8	–	–
ELM	($n = 0$)	($n = 22$)	($n = 321$)	($n = 0$)	($n = 143$)
Baseline sensitivity (dB)	–	7 ± 6	18 ± 8	–	–
Sensitivity change (dB)	–	10 ± 7	2 ± 8	–	–

Investigative Ophthalmology & Visual Science

Table 8. Associations Between Changes in Retinal Sensitivity and Those in Structural Lesions From RVO From Baseline to 6 Month's Follow-up in 6 Patients With RVO (6 Eyes, 453 Points) (Pointwise Mixed-Effect Linear Regression Model)

Term	Estimated Coefficient	Standard Error	*t*-Statistic	*P* Value
Overall mean (intercept)	1.7	2.23	0.76	0.478
Ischemia – developed	−3.65	0.98	−3.71	<0.001
Ischemia – persistent	−2.98	0.81	−3.68	<0.001
Ischemia – resolved	−2.34	1.11	−2.11	0.035
Hemorrhage – developed	7.70	5.43	1.42	0.157
Hemorrhage – persistent	6.24	3.89	1.61	0.109
Hemorrhage – resolved	3.92	0.69	5.68	<0.001
IRF – resolved	1.16	0.596	1.21	0.228
SRF – resolved	2.40	1.04	2.30	0.022

normal values (−2.34 dB) ($P = 0.035$). Resolution of hemorrhage ($n = 114$) was associated with a statistically significant improvement of retinal sensitivity (+7.70 dB; $P < 0.001$), reaching values close to those of control fellow eyes. Locations in which hemorrhage developed ($n = 1$) or persisted ($n = 2$) were rare, giving insufficient power to detect differences. The resolution of SRF ($n = 114$) was associated with some improvement in retinal sensitivity, but the resolution of IRF was not (and +2.40 dB [$P = 0.022$]; +1.16 dB [$P = 0.228$]; respectively). It was not possible to evaluate the effect of the integrity of the IS/OS and ELM because of the very small number of locations affected by these lesions at baseline (absent ELM = 22, absent IS/OS = 3).

Owing to the small number of points with recorded retinal thicknesses (total and GCL-IPL) at follow-up ($n = 108$) (i.e., 18 points [9 points from 2 rows] in each of the 6 eyes with follow-up) corrections for total and GCL-IPL thickness could not be undertaken on the evaluation of changes at the 6-month follow-up.

Discussion

Retinal ischemia, IRF, and SRF were all found to be statistically significantly associated with a reduction in retinal sensitivity. The association persisted when correcting for total or GCL-IPL thickness, suggesting the effect on retinal sensitivity was a direct result of the presence of the RVO lesion itself. Increased total retinal thickness and increased thickness of the GCL-IPL were also associated with decreased retinal sensitivity. Owing to the small number of points with absent IS/OS or ELM, associations between the integrity of these layers and retinal sensitivity could not be determined.

The resolution of SRF led to statistically significant improvements in retinal sensitivity, albeit not to the level observed in corresponding locations in fellow eyes. This finding suggests that either irreversible damage to retinal cells had already occurred when treatment was initiated or functional loss still occurs despite treatment. It is also possible that further improvements in function may have taken place after a longer follow-up. Resolution of retinal ischemia, observed in only 31 of the 486 points with retinal ischemia at baseline studied (6%), did not result in improvements in retinal sensitivity. In fact, further loss of sensitivity still occurred after resolution. To our knowledge, this finding has not been reported previously, but is important. It is possible that reperfusion of the ischemic area may have occurred once cell demise had already taken place. If that were to be the case, this finding would suggest that any therapeutic attempt to achieve retinal reperfusion would need to be initiated very soon after RVO onset to recover retinal function. It would be also possible that the treatment used (anti-VEGF) may not have modified the course and progression of cell damage in areas of ischemia, once initiated. Previous studies on RVO found reperfusion of nonperfused areas occurred in a proportion of patients with CRVO and BRVO after monthly injections of anti-VEGFs.[14,15] Reperfusion, however, was not observed with less frequent administration of anti-VEGFs.[16] The potential beneficial effect of anti-VEGFs in reperfusion may relate to the role of these agents in decreasing retinal capillary leukostasis and opening up retinal capillaries closed by adherent leukocytes.[17]

Very few studies have evaluated point-to-point functional–structural correlates in eyes with RVO[7,9,10,11,13]; only one of these,[13] which was a retrospective, cross-sectional study, included eyes with RVO naïve to treatment. The authors of these studies used less densely interrogated areas, with 29 to 57 points in areas between 5° and 10° when compared with the 81 stimuli in the 8° × 8° square grid we purposely developed for the current study (with a total of 810 points being investigated in RVO eyes). Our more densely tested area is expected to have increased the accuracy of the relationships investigated. Like in our own study, decreased retinal sensitivity was observed in areas of nonperfusion in previous studies.[7,9,13]

The strengths of our study include a detailed evaluation of the relationship between retinal sensitivity and lesions of RVO outside the foveal area, which, to our knowledge, have never been done before. Patients naïve to treatment were evaluated; some were followed longitudinally after treatment with anti-VEGFs, which allowed a determination of the changes in retinal sensitivity occurring after persistence, resolution, or new development of RVO lesions. A customized 8° × 8° grid testing 81 points/locations (i.e., a highly packed area) was interrogated, permitting a detailed evaluation of retinal sensitivity and precise point to point correlation with retinal structure. The study was meticulously conducted to ensure that areas investigated by the different functional and structural diagnostic technologies were at the exact same location. Limitations include the small number of patients assessed and the relatively short follow-up.

Acknowledgments

The authors thank all patients that participated in this study.

Supported by King Abdulaziz University in Rabigh, Saudi Arabia, and the Saudi Arabian Cultural Bureau in London,

United Kingdom (grant number R8384CEM) and by Miss Elizabeth Sloan, to whom the authors are very grateful. Funders had no input in the study design, analysis or interpretation of the data presented herein.

Disclosure: **M. Khayat**, None; **J. Perais**, None; **D.M. Wright**, None; **M. Williams**, None; **N. Lois**, None

References

1. Ehlers JP, Fekrat S. Retinal vein occlusion: beyond the acute event. *Surv Ophthalmol*. 2011;56(4):281–299.
2. Khayat M, Williams M, Lois N. Ischemic retinal vein occlusion: characterizing the more severe spectrum of retinal vein occlusion. *Surv Ophthalmol*. 2018;63(6):816–850.
3. Kriechbaum K, Prager F, Geitzenauer W, Benesch T, Schütze C, Simader C, Schmidt-Erfurth U. Association of retinal sensitivity and morphology during antiangiogenic treatment of retinal vein occlusion over one year. *Ophthalmology*. 2009;116(12):2415–2421.
4. Noma H, Funatsu H, Mimura T, Harino S, Shimada K. Functional-morphologic correlates in patients with branch retinal vein occlusion and macular edema. *Retina*. 2011;31(10):2102–2108.
5. Noma H, Funatsu H, Mimura T, Shimada K. Influence of ischemia on visual function in patients with branch retinal vein occlusion and macular edema. *Clin Ophthalmol*. 2011;5(1):679–685.
6. Noma H, Funatsu H, Mimura T, Shimada K. Visual function and serous retinal detachment in patients with branch retinal vein occlusion and macular edema: a case series. *BMC Ophthalmol*. 2011;11:29.
7. Ota M, Tsujikawa A, Ojima Y, et al. Retinal sensitivity after resolution of the macular edema associated with retinal vein occlusion. *Graefes Arch Clin Exp Ophthalmol*. 2012;250(5):635–644.
8. Mylonas G, Sacu S, Dunavoelgyi R, et al. Response of retinal sensitivity to ranibizumab treatment of macular edema after acute branch retinal vein occlusion. *Retina*. 2013;33(6):1220–1226.
9. Manabe S, Osaka R, Nakano Y, et al. Association between parafoveal capillary nonperfusion and macular function in eyes with branch retinal vein occlusion. *Retina*. 2017;37(9):1731–1737.
10. Ghashut R, Muraoka Y, Ooto S, et al. Evaluation of macular ischemia in eyes with central retinal vein occlusion: an optical coherence tomography angiography study. *Retina*. 2018;38(8):1571–1580.
11. Kadomoto S, Muraoka Y, Ooto S, et al. Evaluation of macular ischemia in eyes with branch retinal vein occlusion. *Retina*. 2018;38(2):272–282.
12. Niro A, Sborgia G, Sborgia A, et al. Analysis of morphologic and functional outcomes in macular edema due to central retinal vein occlusion treated with intravitreal dexamethasone implant. *J Ophthalmol*. 2018;9;5604632.
13. Tomiyasu T, Hirano Y, Suzuki N, et al. Structural and functional analyses of retinal ischemia in eyes with retinal vein occlusion: relationship with macular edema or microaneurysm formation. *Ophthalmic Res*. 2019;61(4):218–225.
14. Mir TA, Kherani S, Hafiz G, et al. Changes in retinal nonperfusion associated with suppression of vascular endothelial growth factor in retinal vein occlusion. *Ophthalmology*. 2016;123:625–634.e1.
15. Campochiaro PA, Bhisitkul RB, Shapiro H, Rubio RG. Vascular endothelial growth factor promotes progressive retinal nonperfusion in patients with retinal vein occlusion. *Ophthalmology*. 2013;120:795–802.33.
16. Sophie R, Hafiz G, Scott AW., et al. Long-term outcomes in ranibizumab-treated patients with retinal vein occlusion; the role of progression of retinal nonperfusion. *Am J Ophthalmol*. 2013;15(6):693–705.
17. Liu Y, Shen J, Fortmann SD, et al. Reversible retinal vessel closure from VEGF-induced leukocyte plugging. *JCI Insight*. 2017;21;2(18):e95530.